Warping Stresses and Deflections in Concrete Pavements: Part III

A. S. REDDY, G. A. LEONARDS, and M. E. HARR, respectively, Research Assistant, School of Civil Engineering; Professor of Soil Mechanics; and Associate Professor of Soil Mechanics, Purdue University

The role of theoretical analyses in the development of reliable design criteria for concrete pavements is reviewed. Available theories are examined in the light of performance records. As the underlying assumptions are incomplete, the usefulness of these theories is limited; moreover, the concepts involved have restricted planning of field experiments to the point where significant variables have not been measured, with the result that interpretation of the data is confused and the findings inconclusive.

A theory is presented which accounts for warping produced by nonlinear temperature and moisture variations of sufficient magnitude to result in a partly supported slab, and the subgrade support characteristics are generalized to include time-dependent deformations. The behavior of concrete pavements predicted by this theory is found to be compatible with field performance; its use as a basis for designing more significant field experiments is recommended.

•ACCORDING to Farrell and Paterick (1), expenditures for all types of surfacing on primary and secondary roads have comprised about 40 percent of the construction funds for highways as compared with about 25 percent, each, for grading and structures. In 1960, about 4,000 miles of new concrete pavements were constructed in the United States (2), an increase of approximately 60 percent over that being constructed during the previous five years. Thus, expenditures for concrete pavements represent an important and increasing fraction of the nation's highway investment. The need for improved design criteria is now more pressing than ever.

DEVELOPMENT OF DESIGN CRITERIA

Over a period of some 50 years, each of the following approaches has aided materially in the development of design procedures for concrete pavements: (a) laboratory experiments, (b) controlled field experiments—test sections and test roads, (c) observations of prototype performance, and (d) theoretical analyses. The relative utility of these techniques will be reviewed briefly.

Highway pavements are among the most complex structures with which the civil engineer has to deal. The loads are variable in magnitude, space, and time, and large numbers of load repetitions must be taken into account; major changes in topography, subgrade materials, ground water and drainage conditions are common; the behavior of layered systems with widely different strength and displacement tolerances must be evaluated; and local variations in climatic conditions affect performance to a greater extent than in virtually any other structure of concern to the civil engineer.

Faced with such variety of significant variables, laboratory tests in which it is feasible to control only a limited number of variables and geometries can be of value primarily for the purpose of elucidating specific phenomena, such as, the effects of

Paper sponsored by Committee on Rigid Pavement Design.

repeated loads on cumulative deflections, the pumping characteristics of various types of subbases, the relative shear strength of subgrade soils, and the effects of compaction. Although such studies are very useful, in the absence of a mechanism for combining the interactions of these properties with other factors affecting pavement performance, laboratory tests are inherently incapable of leading to the formulation of more reliable overall design procedures.

Test sections and test roads permit control of a number of variables under specific prototype conditions. Highway engineers have had the foresight to use this tool to a greater extent than their counterparts in structural and foundation engineering, yet these efforts have not led to the development of generally valid design criteria. This is because prototype conditions vary widely from locality to locality and adequate procedures for translating behavior—and the interactions contingent upon this behavior—from one locality to another are not yet available. Perhaps the most valuable aspect of a test road is its use to assess the validity of a design procedure. Comparisons of this nature have almost invariably demonstrated that large disparities exist between predicted and observed behavior. It is still widely believed that the stronger the support beneath a concrete pavement the better the performance of the pavement for a given set of loading conditions. Table 1 is an abbreviated summary of the rigid pavement survival data obtained at the AASHO Road Test (3). It is apparent that subbase thickness had a minor influence on performance. In contrast to the behavior of flexible pavements, single-axle loads were hardly more damaging than their (theoretically) equivalent tandem-axle loads, but what assurance can be given that this will also be the case under a different set of prototype conditions? On the other hand, if an analysis were available that could predict such performance, and this prediction could be verified in a test road under another set of conditions, designs for other environments and loading arrangements could subsequently be made with confidence. These considerations illustrate the strength and weaknesses of the test road approach in furthering the development of reliable design concepts.

Observation of prototype performance still remains a primary basis of pavement design procedures. Investigation of failures has led to a gradual evolution in design practices so that today satisfactory pavements can be constructed to suit local conditions almost anywhere in the United States. However, this approach has many drawbacks. In the 1940's, when vehicle loads and numbers were increasing rapidly, experience could not keep pace with changing conditions. The situation has been partly remedied by enacting laws to limit vehicle loads, yet evidence is lacking to the effect

TABLE 1

ABBREVIATED SUMMARY OF PERFORMANCE DATA, NONREINFORCED CONCRETE PAVEMENTS AT AASHO ROAD TEST

Loop	Axle Load (kips)	Subbase Thickness (in.)	Axle Applications (1,000's) to Failure[a]					
			5-In. Surface	6½-In. Surface	8-In. Surface	9½-In. Surface	11-In. Surface	12-In. Surface
3	12S	3	(3.7)	(3.9)	(4.4)			
		6	(3.1)	(4.1)	(4.3)			
		9	(3.7)	(4.2)	(4.0)			
	24T	3	705	(4.0)	(4.3)			
		6	901	(4.1)	(4.3)			
		9	771	(4.0)	(4.2)			
4	18S	3	716	(3.8)	(4.5)	(4.2)		
		6	353	(4.3)	(4.4)	(4.5)		
		9	291	(3.0)	(4.3)	(4.1)		
	32T	3	343	687	(4.2)	(4.0)		
		6	328	1,000	(4.2)	(4.2)		
		9	289	722	(4.1)	(4.2)		
5	22.4S	3		760	(4.2)	(4.3)	(4.1)	
		6		898	(4.1)	(3.7)	(4.5)	
		9		705	1,111	(4.5)	(4.5)	
	40T	3		335	(4.2)	(4.2)	(4.3)	
		6		369	(4.2)	(4.0)	(4.5)	
		9		698	898	(3.8)	(4.4)	
6	30S	3			878	(3.6)	(4.4)	(4.2)
		6			(3.9)	(4.3)	(4.2)	(4.0)
		9			(3.4)	(4.2)	(4.3)	(4.2)
	48T	3			(1.8)	(3.1)	(4.3)	(4.3)
		6			(4.1)	(4.3)	(4.3)	(4.2)
		9			1,114	(4.3)	(4.3)	(4.4)

[a] Failure is taken at a serviceability index of 1.5. Numbers in parentheses are serviceability indices at end of test (no failure). S = single axle, T = tandem axle.

that current legal restrictions represent an optimum combination of road costs and vehicle efficiency and experiments with vehicle design (as related to pavement design) have been greatly restricted. Furthermore, due to changes in local conditions, virtually every state uses a different design procedure, hampering exchanges in experience between states and greatly limiting the possibilities of utilizing 50 years of road-building experience in this country in the design of equally satisfactory roads abroad. Most serious of all, although a number of current designs have proven satisfactory, there is no basis for deciding that they are necessarily the most economical. Some recent designs have been disappointing, and proposals for radical changes in pavements sections, such as the use of insulating layers for the purpose of attenuating the detrimental effects of frost action, cannot be fully accepted until a record of satisfactory performance based on trial and error techniques has been developed.

It is apparent, therefore, that the lack of adequate theory has been the largest single factor hampering further progress in highway pavement design. The validity of a theory can readily be assessed, partly in the laboratory, but principally by the use of test sections or by observations of prototype behavior. If a theory embraces the significant aspects of the problem, it can form the strongest link possible for translating experience from one locality to another. No restrictions need be placed on changing conditions, and the most economical (yet satisfactory) design can quickly be arrived at for any specific set of conditions. The history of technological development in every area of human endeavor bears eloquent testimony to the validity of these facts. A sustained and concerted effort to develop more reliable theories of pavement design is urgently needed if the public is to receive the fullest possible benefits from its highway dollar.

REVIEW OF AVAILABLE THEORIES

In earlier papers (4, 20,), the factors that influence the performance of concrete pavements were reviewed. Although it was recognized that the development of cracks in concrete pavements was not necessarily indicative of impending failure, cracks in existing roads generally reflect deficiencies in design and construction practices. The occurrence of these cracks may not be injurious initially from the standpoint of driving comfort, but rather from the danger of water penetration (and subsequent loss of support), from the loss of effective load transfer and reduced mass of the individual slabs, and from the danger of spalling and increased pavement deterioration. The gradual elimination of diagonal (corner) and longitudinal cracks in concrete pavements was traced, and it was shown that (except in special cases) failure of modern concrete pavements could not be attributed to weak subgrade support, pavement pumping, frost action, poor load transfer at joints, or deterioration of unsound concrete. Extensive performance data were cited to show that by far the major proportion of cracks were oriented transversely to the direction of the road and that they were caused primarily by the combined effects of pavement warping and superimposed traffic loads. Unequivocal evidence was presented to the effect that, for typical ambient conditions, variations in temperature and moisture with slab thickness induced warping of sufficient magnitude to result in partially supported slabs.

Although Goldbeck (5) in 1919 and Older (6) in 1921 independently derived a "corner formula" for the required thickness of concrete pavement slabs (to account for loss of support at the corners due to weak subgrades and temperature and moisture differentials), the first completely rational theoretical analysis was contributed by Westergaard (7) in 1926. In 1927 Westergaard (8) extended his analysis to the consideration of stresses and deflections induced in the slab by uniform temperature gradients. With modifications to account for the effects of adjacent loads (9), impact (10), load repetitions (11, 12) and warping effects (10, 11, 13, 14, 15), Westergaard's analysis still serves as a framework around which current design procedures for concrete pavements are built. It is pertinent, therefore, to review the basic assumptions made in this theory; namely, (a) that the temperature gradients are uniform, (b) that the slab remains at all times in full contact with its support, and (c) that the support can be represented by independent elastic springs of constant stiffness, as suggested earlier by Winkler (16).

The consequences of these assumptions has been the development of a conceptionally inadequate basis for predicting the behavior of concrete pavements. They suggest that the critical stresses will produce diagonal cracks at the corners, whereas the majority of cracks are now transverse. They indicate that, for a given set of conditions, an increase in subgrade modulus would permit the use of a reduced slab thickness, whereas it has been known for some time that concrete pavements placed on rock break up rapidly. The general lack of correlation between subgrade modulus and pavement performance is now well documented (3). Moreover investigations to evaluate the behavior of concrete pavements have generated considerable confusion, as deflections and strains have been measured without full knowledge of the actual support conditions at the time the measurements were taken.

In 1959, Harr and Leonards (4, 40) solved the "slab on ground" problem to include the (more common) case where warping due to temperature and/or moisture gradients results in partly supported slabs. For the first time, it was shown analytically that high values of the subgrade modulus (K) can result in increasing (rather than decreasing) critical stresses due to warping and that interactions between slab size and thickness, degree of subgrade support, and concrete quality may result in either increasing or decreasing critical (tensile) stresses with increasing values of K. However, the concept of a subgrade modulus (Winkler foundation), and the assumption of a uniform temperature gradient was retained.

The Winkler type foundation lacks continuity in the medium (shear stresses are neglected) and poses severe problems in determining appropriate values of K (17). For this reason, a number of investigators have preferred to replace the Winkler foundation with an elastic continuum (18). Hetenyi (19) observed: "Though the first type [Winkler foundation] is mathematically simpler, one should not regard it, as some investigators do, as an approximate or elementary solution for the elastic solid foundation, because of its own physical characteristics and significance."

Full scale experiments (20) on a slab warped by temperature gradients to a condition of partial support corroborate this view for short-term loadings. However, under sustained loadings (such as the weight of the slab), most subgrade soils suffer time-dependent deformations due to consolidation or creep processes, or to a combination of these factors. (Depending on the relative rates of these processes, creep in the concrete slab may also be important.) Such time-dependent deformations may be simulated by viscoelastic models (21, 22).

A variety of mechanical models has been proposed (23) to simulate the behavior of the viscoelastic materials. These generally consist of various combinations of three fundamental types: (a) Maxwell element, (b) Kelvin element and (c) standard solid element (Fig. 1). Freudenthal and Lorsch (24) discussed the three mechanical models and compared the behavior of these models with the actual behavior of soil. Graphs were presented to indicate that the standard solid model gives the best approximation to the actual behavior of soil.

For problems whose geometry does not vary with time, the time dependency of the viscoelastic problem can be removed by taking the Laplace transform of the differential equations and boundary conditions. This operation transforms the viscoelastic problem into an elastic problem, and the inverse transform of the solution gives the solution to the viscoelastic problem. Using this method, Freudenthal and Lorsch (24) solved the problem of an infinite beam on a viscoelastic foundation; Hosken and Lee (25) solved the problem of an infinite elastic plate on a viscoelastic foundation; Pister and Williams (26) solved the problem of an infinite plate on a viscoelastic foundation taking into account Reissner's (27) shear interactions; and Kerr (28) solved the problem of a rigid circular plate on a viscoelastic foundation taking into account shear interactions. Lee (29), and Boley and Weiner (30), discuss other methods of solving viscoelastic problems and include excellent bibliographies. For the special case where the slab is in full contact with its support, the principle of superposition may be applied and the use of the Laplace transform method is justified. However, for the more common case of partial support, superposition is not applicable (even though the differential equations are linear) because each component of loading has an independent effect on the distance to the point of zero support (Fig. 2).

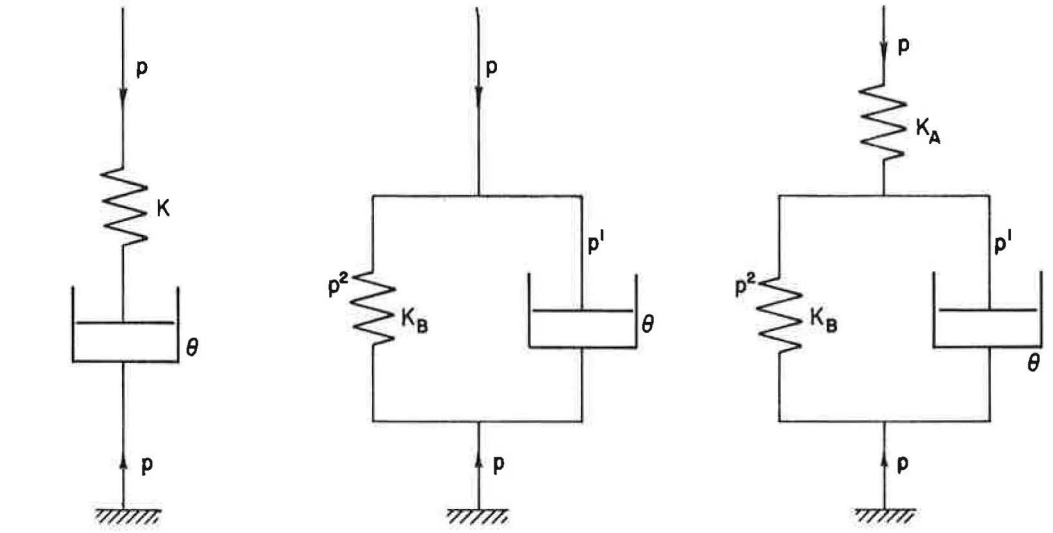

Figure 1. Basic elements of viscoelastic models.

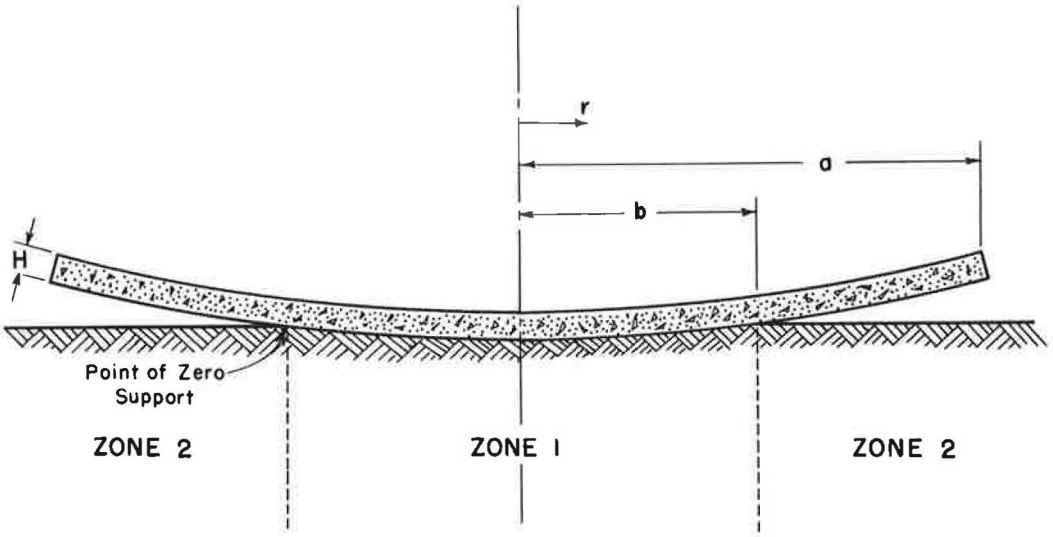

Figure 2. Simplified diametral section of a warped slab.

In their solution of the partly supported slab on a Winkler foundation Harr and Leonards (4, 20) assumed linear temperature (or moisture) variations through the thickness of the slab, although observations by Teller and Sutherland (15), Lang (31), and the Corps of Engineers (32) showed that curved temperature variations represent the more usual distribution. This was based on the fact that Teller and Sutherland concluded from their observations that linear variations are more critical, and the fact that Thomlinson's analysis (33) of a simple harmonic variation in temperature at the top surface of the slab (which resulted in curved temperature variations) gave values of computed stresses less than those of Westergaard for a fully supported slab. However, once the solution to a partly supported slab on a viscoelastic foundation was ob-

tained, it was realized that non-linear temperature (or moisture) variations could be more critical than linear variations.

In summary, realistic analysis of the critical stresses and deflections that develop in concrete slabs on ground due to their weight, superimposed loads, and temperature (and/or moisture) variations must take into account at least the following three physical phenomena:

1. Warping of sufficient magnitude to result in only partial support of the slab by the ground;
2. Non-linear temperature (and/or moisture) variations as a function of slab thickness; and
3. Subgrade reactions that are time-dependent.

This report presents an analysis that includes all three of these factors. Numerical solutions were obtained for the Maxwell and standard solid models for linear (equivalent) temperature variations, and for the case where the temperature variations can be represented by the combination of a linear and a (symmetrically) curved variation. Comparisons are made with the solutions obtained by Leonards and Harr (4) and with field performance records. On the basis of these comparisons, the utility of the new theory is assessed.

THEORY

Assumptions

1. Homogeneous, isotropic, circular slab with a free edge boundary obeying Hooke's law.
2. The supporting medium is homogeneous and is represented at each point of contact by an independent viscoelastic element.
3. Deflections of the slab are small in comparison to its thickness.
4. External forces acting on the slab are those due to gravity and/or a uniformly distributed load acting normal to the surface of the slab. Inertia forces are neglected.
5. The slab is subjected to a temperature (and/or moisture) variation with depth that is independent of time. The variation in temperature is constant on all planes parallel to the upper and lower slab surfaces.

Notation

F = force
L = length
T = temperature
t = time
w = deflection, considered positive in the upward direction (L)
$w_{m,n}$ = deflection at the nodal point n after mth increment in the value of the radial distance to the point of zero deflection (L)
E = Young's modulus (F/L^2)
μ = Poisson's ratio
H = slab thickness (L)
y = any arbitrary distance from the center of the slab, positive down (L)
q = uniformly distributed load due to the weight of the slab and/or surface loading (F/L^2)
$D = \frac{E\,H^3}{12\,(1-\mu^2)}$ = flexural rigidity of the slab (FL)

$T(y)$ = temperature at depth y (T)
ΔT = temperature difference between top and bottom of slab
K = spring constant for Winkler foundation or Maxwell model (F/L^3)
K_A = spring constant of upper spring in standard solid model (F/L^3)
K_B = spring constant of lower spring in standard solid model (F/L^3)
$p(t)$ = upward reaction on the slab at time t (F/L^2)

$p^1(t)$ = reaction on dash pot at time t (F/L^2)
$p^2(t)$ = reaction on lower spring in standard solid model at time t (F/L^2)
θ = dash pot constant (Ft/L^3)
τ = dimensionless time factor (Kt/θ)
α = linear coefficient of thermal expansion (T^{-1})
λ = distance between two nodal points (L)
r = radial distance (L)
b = radial distance to point of zero deflection (L)
a = radius of slab (L)
t_m = time required for the mth increment in the value of b (t)
V (r) = shear at point r (F/L)
M (r) = radial bending moment at point r (FL/L)
σ (r) = radial stress at point r (F/L^2)

$$\nabla^2 r = \frac{\partial^2}{\partial r^2} + \frac{1}{r}\frac{\partial}{\partial r}$$

$$\nabla^4 r = \left(\frac{\partial^2}{\partial r^2} + \frac{1}{r}\frac{\partial}{\partial r}\right)\nabla^2 r$$

Analysis

The thermoelastic problem is first reduced to an equivalent elastic problem with initial and boundary stresses. Consider a slab that is initially at a uniform temperature. Let the temperature at any distance y from the center of the slab be changed by T (y). Stresses will be applied at the boundary to prevent deformations from occurring within the slab due to the change in temperature. For the strains at all points to be zero (30):

$$\frac{1}{E}(\sigma_r - \mu\sigma_\theta) + \alpha T(y) = 0 \qquad (1a)$$

$$\frac{1}{E}(\sigma_\theta - \mu\sigma_r) + \alpha T(y) = 0 \qquad (1b)$$

From Eqs. 1a and 1b,

$$\sigma_r = \frac{-\alpha E T(y)}{(1-\mu)} = \sigma_\theta \qquad (2)$$

Inasmuch as σ_r and σ_θ are equal, the values of the stresses in any other direction must also equal σ_r.

Thus, to prevent deformations at all points within the slab, stresses σ_r and σ_θ given by Eq. 2 must be applied at every point within the slab and at the boundary of the slab. However, since the boundary at r = a was initially assumed to be free, the radial stress $\frac{-\alpha E T(y)}{(1-\mu)}$ must be removed at the boundary. This can be done conveniently by substituting a statically equivalent force system (which has the same resultant force and moment per unit length) along the boundary but of opposite sign. The thermoelastic problem is reduced to an elastic problem with a moment at r = a and initial stresses at all values of r given by

$$M(r)\Big]_{r=a} = \frac{\alpha E}{(1-\mu)} \int_{-H/2}^{+H/2} T(y)\, y\, dy \qquad (3)$$

$$\sigma_r \text{ (initial)} = \frac{-\alpha E\, T(y)}{(1 - \mu)} + \frac{\alpha E}{H(1 - \mu)} \int_{-H/2}^{+H/2} T(y)\, dy \tag{4}$$

Invoking Saint-Venant's principle (30, 34), the solution obtained using this substitution is very accurate at distances from the free edge larger than the thickness of the slab.

The case where temperature increases with the depth of the slab (upward warping) is treated in this paper. The slab is divided into zones as shown in Figure 2. Zone 1 represents the region that is in contact with the viscoelastic foundation. Zone 2 represents the region having no contact with the foundation.

The differential equation for zone 1 is (35)

$$D\left(\frac{\partial^4 w}{\partial r^4} + \frac{2}{r}\frac{\partial^3 w}{\partial r^3} - \frac{1}{r^2}\frac{\partial^2 w}{\partial r^2} + \frac{1}{r^3}\frac{\partial w}{\partial r}\right) = q - p\,(t) \tag{5}$$

in which q is the superimposed axisymmetrical load and p (t) is the time-dependent subgrade reaction.

The differential equation for zone 2 is (35)

$$D\nabla^4 w = q \tag{6}$$

For the Maxwell model, p and w are related by

$$\frac{\partial w}{\partial t} = \frac{1}{K}\frac{\partial p}{\partial t} + \frac{p}{\theta} \tag{7}$$

For the standard solid model they are related by

$$\frac{\partial w}{\partial t} = \frac{1}{K_A}\frac{\partial p}{\partial t} + \frac{1}{K_B}\frac{\partial p^2}{\partial t} \tag{8a}$$

or

$$\frac{\partial w}{\partial t} = \frac{1}{K_A}\frac{\partial p}{\partial t} + \frac{p^1}{\theta} \tag{8b}$$

The equivalent elastic problem is solved by the finite-difference method. The central difference equations (36, 37) for the first four partial derivatives are (λ, the distance between nodal points):

$$\frac{\partial}{\partial r} \cong \frac{\cdots}{2\lambda} \qquad (-1)\;(0)\;(+1)$$

$$\frac{\partial^2}{\partial r^2} \cong \frac{\cdots}{\lambda^2} \qquad (1)\;(-2)\;(1)$$

$$\frac{\partial^3}{\partial r^3} \cong \frac{\cdots}{2\lambda^3} \qquad (-1)\;(2)\;(0)\;(-2)\;(1)$$

$$\frac{\partial^4}{\partial r^4} \cong \frac{\cdots}{\lambda^4} \qquad (1)\;(-4)\;(6)\;(-4)\;(1) \tag{9}$$

A difference equation will be obtained for each of the interior points within zones 1 and 2. It is apparent from Eq. 5 that a singularity occurs at r = 0. The difficulty is overcome by writing the differential equation in rectangular coordinates,

$$\frac{\partial^4 w}{\partial x^4} + \frac{2\partial^4 w}{\partial x^2 \partial y^2} + \frac{\partial^4 w}{\partial y^4} = \frac{q}{D} - \frac{p(t)}{D} \tag{10}$$

Taking the same origin for both polar and rectangular coordinates, due to radial symmetry at r = 0,

$$\frac{\partial w}{\partial x} = \frac{\partial w}{\partial y} = \frac{\partial w}{\partial r} \tag{11a}$$

$$\frac{\partial^2 w}{\partial x^2} = \frac{\partial^2 w}{\partial y^2} = \frac{\partial^2 w}{\partial r^2} \tag{11b}$$

$$\frac{\partial^4 w}{\partial x^4} = \frac{\partial^4 w}{\partial y^4} = \frac{\partial^4 w}{\partial x^2 \partial y^2} = \frac{\partial^4 w}{\partial r^2} \tag{11c}$$

Therefore

$$4\frac{\partial^4 w}{\partial x^4} = \frac{q}{D} - \frac{p(t)}{D} \text{ (at } r = 0) \tag{12a}$$

or

$$4\frac{\partial^4 w}{\partial r^4} = \frac{q}{D} - \frac{p(t)}{D} \text{ (at } r = 0) \tag{12b}$$

$$M_r = D\left(\frac{\partial^2 w}{\partial r^2} + \frac{\mu}{r}\frac{\partial w}{\partial r}\right) \tag{13a}$$

As $r \to 0$, $\frac{1}{r}\frac{\partial w}{\partial r} \to \frac{\partial^2 w}{\partial r^2}$

Therefore

$$M_r\Big]_{\text{at } r = 0} = D(1 + \mu)\frac{\partial^2 w}{\partial r^2} \tag{13b}$$

There are (n + 3) unknowns (Fig. 3); one nodal point at r = 0, n nodal points in the slab, and 2 nodal points representing the boundary conditions; n equations are obtained from interior points. At the boundary, two additional equations are obtained. For the nodal point that is common to zones one and two, another equation is obtained by equating the difference equations for the common point. (Alternately, the summation of vertical forces may be equated to zero (38). However, consideration of the difference equation for the nodal point common to zones 1 and 2 is much simpler from the standpoint of obtaining numerical results on the computer.) Therefore there are as many equations as unknowns.

If n is the nth nodal point, and using the sign conventions as shown in Figure 3,

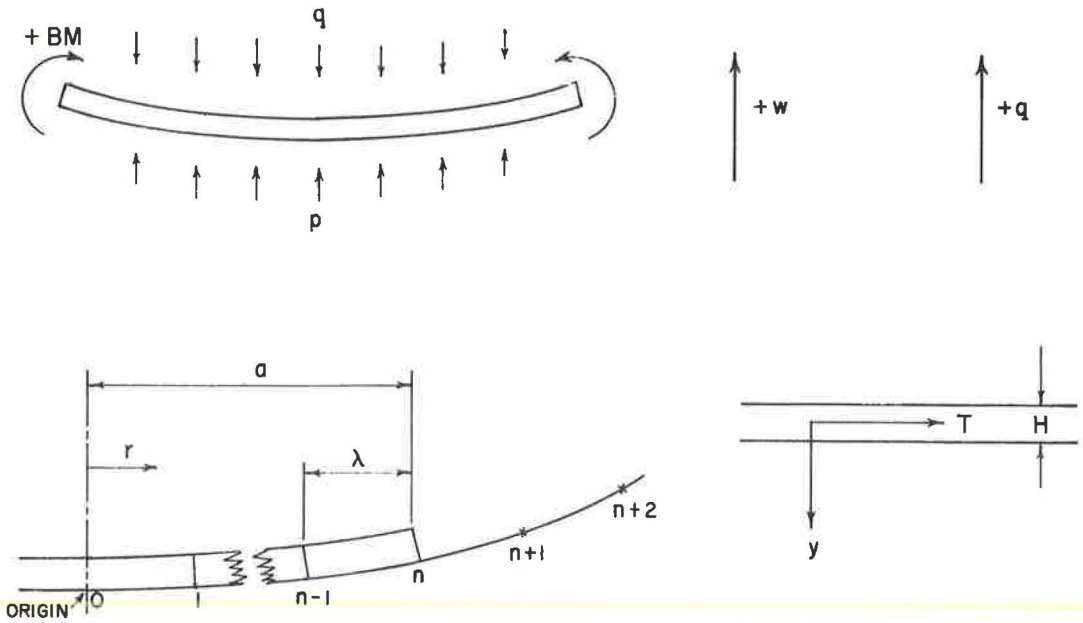

Figure 3. Nomenclature and sign convention for finite difference procedure.

$$\frac{\partial w}{\partial r} \cong \frac{w_{n+1} - w_{n-1}}{2\lambda} \tag{14a}$$

$$\frac{\partial^2 w}{\partial r^2} \cong \frac{w_{n+1} - 2w_n + w_{n-1}}{\lambda^2} \tag{14b}$$

$$\frac{\partial^3 w}{\partial r^3} \cong \frac{w_{n+2} - 2w_{n+1} + 2w_{n-1} - w_{n-2}}{2\lambda^3} \tag{14c}$$

$$\frac{\partial^4 w}{\partial r^4} \cong \frac{w_{n+2} - 4w_{n+1} + 6w_n - 4w_{n-1} + w_{n-2}}{\lambda^4} \tag{14d}$$

Taking the downward loading as q for zones 1 and 2:

$$D\ (\nabla^4 w) = -\ q + p\,(t) \tag{15}$$

For any nth nodal point the difference equations are given by

$$\frac{D}{2n^3\lambda^4}\Big[w_{m,\,n+2}\ (2n^3 + 2n^2) + w_{m,\,n+1}\ (-8n^3 - 4n^2 - 2n + 1) + w_{m,\,n}\ (12n^3 + 4n) + w_{m,\,n-1}\ (-8n^3 + 4n^2 - 2n - 1) + w_{m,\,n-2}\ (2n^3 - 2n^2)\Big] = -\ q + p_{m,\,n} \tag{16}$$

where m is the mth increment in the value of b, the common point for zones 1 and 2. For zone 2, p = 0 and for zone 1, p is a function of time.

The relation of p with deflection and time for a Maxwell element is given by Eq. 7. Writing the difference equation for this relation,

$$\frac{w_{m,n} - w_{m-1,n}}{\Delta t_m} = \frac{1}{K}\frac{(p_{m,n} - p_{m-1,n})}{\Delta t_m} + \frac{p_{m,n}}{\theta} \tag{17}$$

where $p_{m,n}$ is the contact pressure at the nth nodal point after mth increment of b and Δt_m is the time required for increasing b from (m-1)th increment to mth increment. Therefore,

$$K(w_{m,n} - w_{m-1,n}) = (p_{m,n} - p_{m-1,n}) + \frac{K\Delta t_m}{\theta} p_{m,n} \tag{18a}$$

$$K(w_{m,n} - w_{m-1,n}) = p_{m,n}\left(1 + \frac{K\Delta t_m}{\theta}\right) - p_{m-1,n} \tag{18b}$$

$$p_{m,n} = \frac{K(w_{m,n} - w_{m-1,n}) + p_{m-1,n}}{\left(1 + \frac{K\Delta t_m}{\theta}\right)} = \frac{Kw_{m,n}}{\left(1 + \frac{K\Delta t_m}{\theta}\right)} - \frac{Kw_{m-1,n}}{\left(1 + \frac{K\Delta t_m}{\theta}\right)} + \frac{p_{m-1,n}}{\left(1 + \frac{K\Delta t_m}{\theta}\right)} \tag{18c}$$

At $t = 0$, that is, for $m - 1 = 0$, $Kw_{o,n} = p_{o,n}$ (initial condition).

The relation of p with deflection and time of the standard solid element is given by Eqs. 8a and b. Proceeding in the same manner as for the Maxwell element (38)

$$p_{m,n} = \frac{K_A w_{m,n}}{1 + \frac{K_A}{K_B}\left(\frac{K_B\Delta t_{m/\theta}}{1 + \frac{K_B\Delta t_m}{\theta}}\right)} + \frac{\left(p_{m-1,n} - K_A w_{m-1,n}\right)}{1 + \frac{K_A}{K_B}\left(\frac{K_B\Delta t_{m/\theta}}{1 + \frac{K_B\Delta t_m}{\theta}}\right)} + \frac{K_A}{K_B} p^2_{m-1,n} \frac{\left(K_B\Delta t_{m/\theta}\right) \Big/ \left[1 + \left(K_B\Delta t_{m/\theta}\right)\right]}{1 + \frac{K_A}{K_B}\left(\frac{K_B\Delta t_{m/\theta}}{1 + \frac{K_B\Delta t_m}{\theta}}\right)} \tag{19}$$

At t = 0, that is, for m - 1 = 0, $p^2_{o,n} = 0$ (initial condition).

Difference Equations for Boundary Conditions

For the shear at r = a to be zero,

$$- D \frac{\partial}{\partial r} (\nabla^2 w) = 0 \tag{20a}$$

or

$$- D \left[\frac{\partial^3 w}{\partial r^3} - \frac{1}{r^2} \frac{\partial w}{\partial r} + \frac{1}{r} \frac{\partial^2 w}{\partial r^2} \right]_{r = a} = 0 \tag{20b}$$

for which the difference equation is (n = a/λ),

$$- D \left[\frac{w_{m, a/\lambda+2} - 2w_{m, a/\lambda+1} + 2w_{m, a/\lambda-1} - w_{m, a/\lambda-2}}{2\lambda^3} - \right.$$

$$\frac{1}{a^2} \frac{(w_{m, a/\lambda+1} - w_{m, a/\lambda-1})}{2\lambda} +$$

$$\left. \frac{1}{a} \frac{(w_{m, a/\lambda+1} - 2w_{m, a/\lambda} + w_{m, a/\lambda-1})}{\lambda^2} \right] = 0 \tag{21}$$

For the moment at r = a to be M_o, as given by Eq. 3

$$D \left(\frac{\partial^2 w}{\partial r^2} + \frac{\mu}{r} \frac{\partial w}{\partial r} \right) r = a = M_o \tag{22}$$

for which the difference equation is

$$D \left[\frac{(w_{m, a/\lambda+1} - 2w_{m, a/\lambda} + w_{m, a/\lambda-1})}{\lambda^2} + \right.$$

$$\left. \frac{\mu}{2a\lambda} \frac{(w_{m, a/\lambda+1} - w_{m, a/\lambda-1})}{\lambda^2} \right] = M_o \tag{23}$$

RESULTS

Computation Procedures

It is more convenient to work with increments in b, the radial distance to the point of zero deflection and to calculate the corresponding time increment Δt rather than to work directly with increments in time. In order to reduce the number of variables involved, the solutions are presented in terms of a dimensionless "time factor."

For the Maxwell model:

$$\tau = \frac{K}{\theta} \Delta t \tag{24}$$

For the standard solid model:

$$\tau = \frac{K_B \Delta t}{\theta} \tag{25}$$

The corresponding time increments can be obtained from a knowledge of the relaxation time, K/θ.

The starting point in the computations (t = 0) is the solution for a Winkler foundation (4). From this value of b, the first increment in b is taken to the immediately adjacent nodal point; thereafter, the increments in b equal the nodal point spacing λ. A decision must be made regarding the number of nodal points to be used in the numerical solution. The number must be large enough to give sufficiently precise results but not so large as to make the computational procedure too cumbersome. Furthermore, the value of λ must be small enough so that data can be obtained for a sufficient number of τ-values to show the effects of the viscoelastic foundation as a function of time.

For a = 240 in., a value of λ = 5 in. was selected; that is, a = 48 λ. Thus, the total number of nodal points is 48 + 1, the nodal point at r = 0. With the two difference equations representing the boundary conditions, the total number of simultaneous equations to be solved is 51. A flow diagram (Fig. 4) for the FORTRAN source program (39) is used in the solution; the complete program is given by Reddy (38). To examine the precision of the result, a comparison of the deflection and stress at r = 0 for a = 48 λ (51 equations), and a = 96 λ (99 equations), is given in Table 2. It is apparent that λ = 5 in. is a sufficiently small increment to give more than adequate precision for practical purposes.

Numerical Results

Due to the large number of variables involved, it is impractical to present the results as an assembly of charts similar to those prepared by Harr and Leonards (4) for the Winkler foundation. Numerical results are available (38) for the following combination of data for the case of linear variation in temperature with depth: a = 240 in.; H = 4, 12, and 24 in.; μ = 0.15; $\alpha = 6 \times 10^{-6}$ in./in./°F; ΔT = 30 F; and $E = 3 \times 10^6$ and 5×10^6 psi.

For the Maxwell model the values of K selected equal 100, 200, 400, and 700 pci; for the standard solid model computations were made for the ratio K_A/K_B equal to 0.5, 1.0, 3.0, and 10.0 with K_A = 100, 200, 400, and 700 pci.

For illustrative purposes, sets of three curves giving the deflection, radial stress at upper surface of slab, and subgrade reaction as a function of radius and time factor for a few combinations of the parameters listed above are shown in Figures 5 through 10. In spite of an extensive search of the literature, values of relaxation time K/θ appropriate to this problem were not found. Therefore, interpretation of the results in terms of actual times must await experimental determination of K/θ-values.

If the temperature distribution is nonlinear the procedure is the same, except that the initial stresses and deflections (at τ = 0) must be determined for the case of a slab on Winkler foundation with initial stresses and end moments as given by Eqs. 3 and 4 (40). If the temperature distribution can be approximated by

$$T(y) = A\, y^{2k} + B\, y \tag{26}$$

where, A and B are constants and k is any positive integer, the solution is greatly simplified. Eq. 26 can be separated into two parts:

$$T = B\, y \tag{27}$$

$$T = A\, y^{2k} \tag{28}$$

Eq. 27 represents a linear temperature distribution whose solution has already been

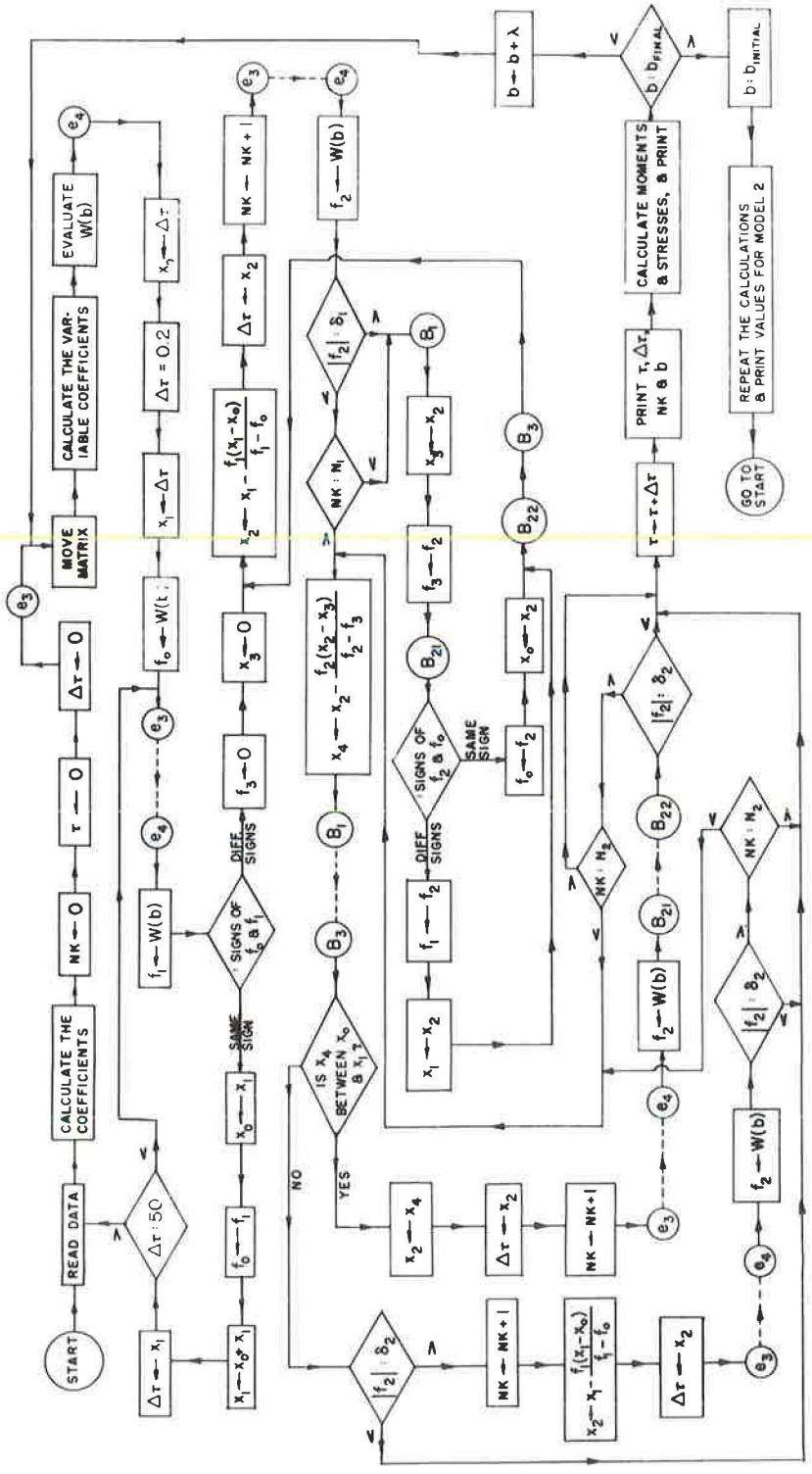

Figure 4. Flow diagram.

TABLE 2

COMPARISON OF DEFLECTIONS AND TENSILE STRESS AT r = 0

b (in.)	Time Factor		Deflection (in. × 10^{-3})		Stress (psi)	
	λ = 5 In.	λ = 2.5 In.	λ = 5 In.	λ = 2.5 In.	λ = 5 In.	λ = 2.5 In.
175	0.3204	0.3200	2.000	1.973	527.0	526.9
180	1.540	1.536	3.388	3.389	529.5	528.8
185	3.560	3.586	5.697	5.633	538.6	538.0
190	6.662	6.68	9.839	9.573	555.4	556.3
195	11.01	11.11	17.40	16.93	576.8	580.0
200	17.07	17.17	30.39	29.76	597.3	602.0
205	25.22	25.28	50.96	50.24	611.7	616.8
210	36.02	36.03	81.29	80.74	616.9	621.7
215	50.14	50.10	123.5	123.4	611.6	615.4
220	68.41	68.38	179.7	180.5	595.3	597.8

Maxwell model: K = 200 pci; a = 240 in.; E = 5,000,000 psi; ΔT = 30F; and H = 4 in.

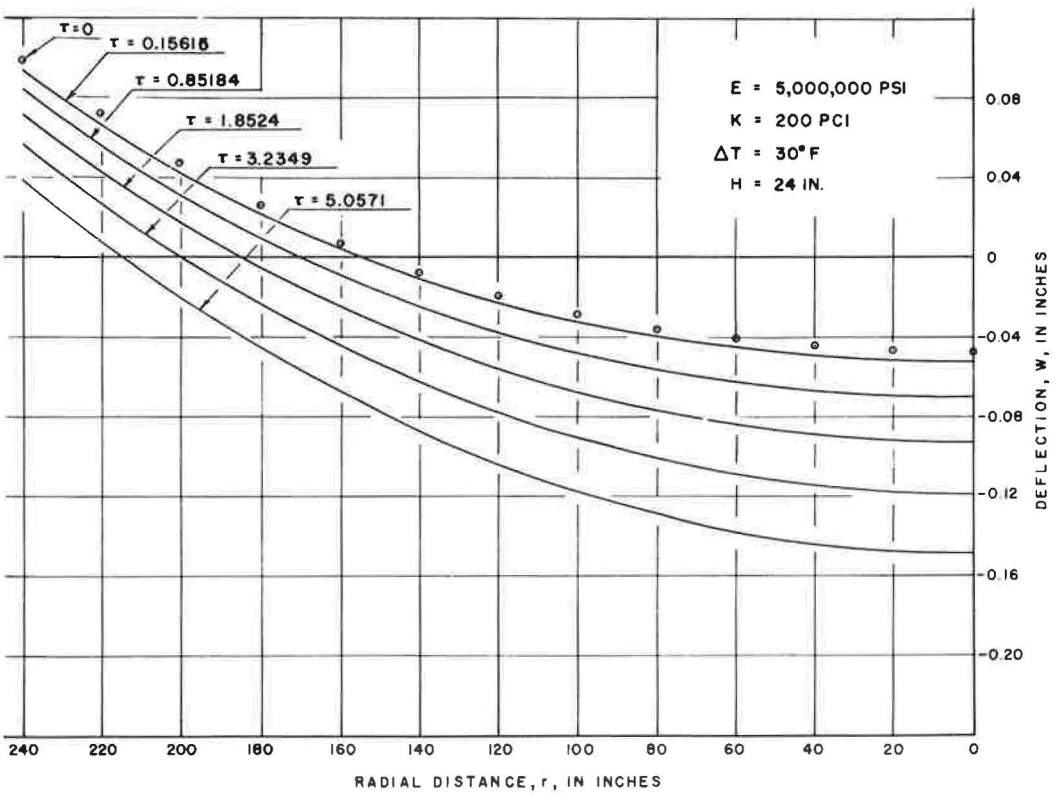

Figure 5. Deflection curves for slab on Maxwell foundation.

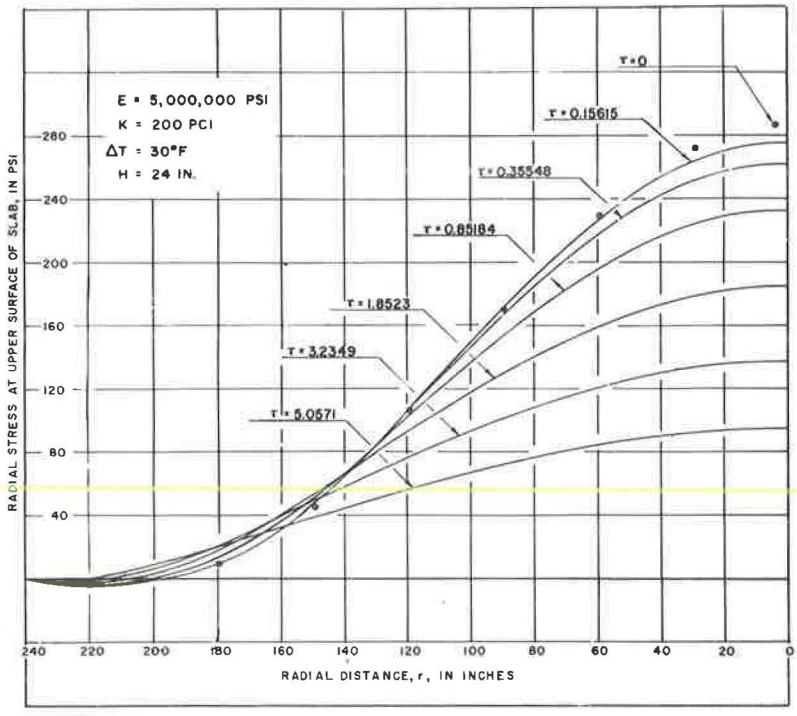

Figure 6. Radial stresses for slab on Maxwell foundation.

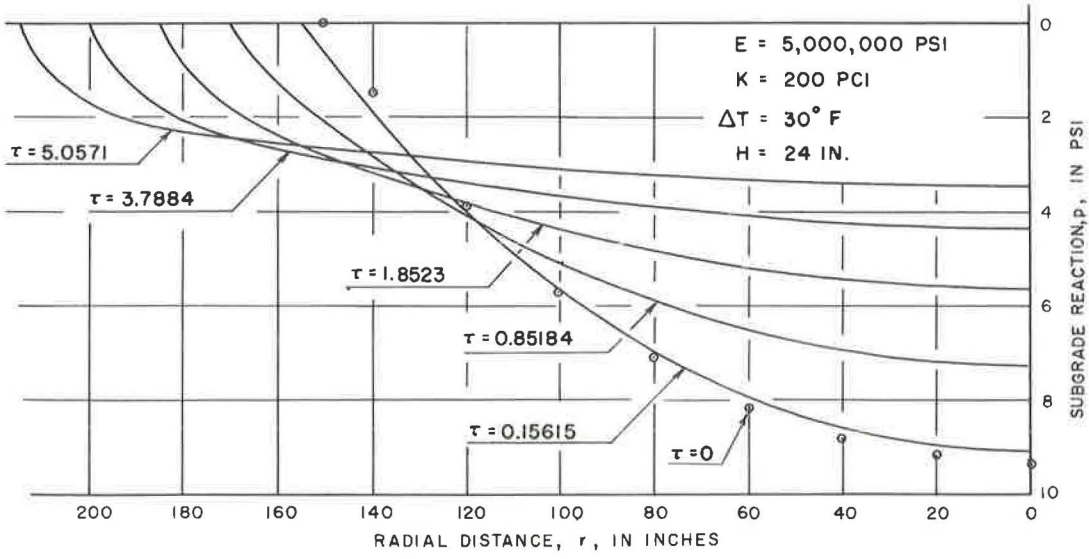

Figure 7. Subgrade reaction for slab on Maxwell foundation.

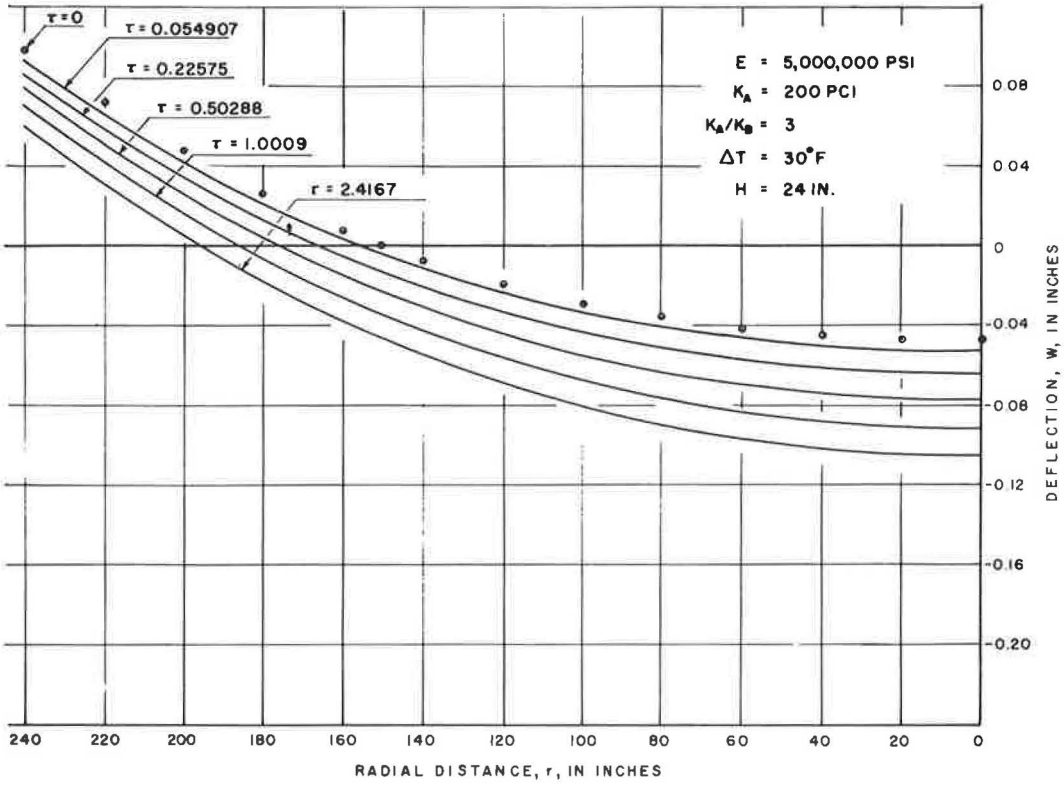

Figure 8. Deflection curves for slab on standard solid foundation.

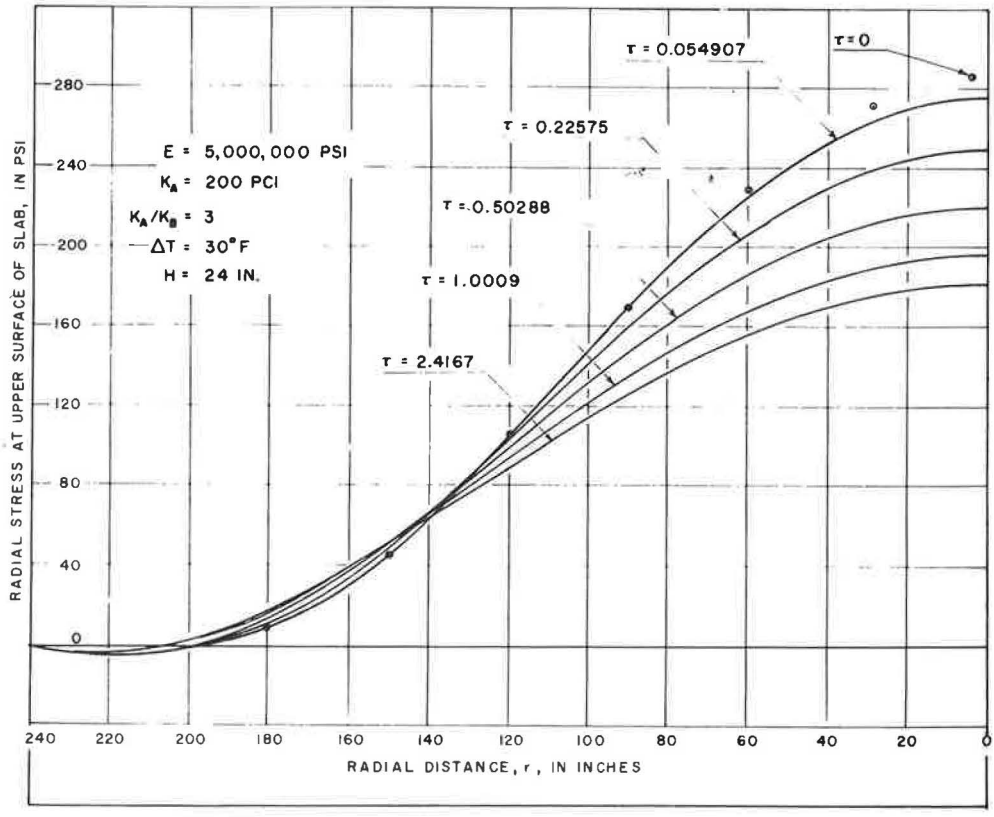

Figure 9. Radial stresses for slab on standard solid foundation.

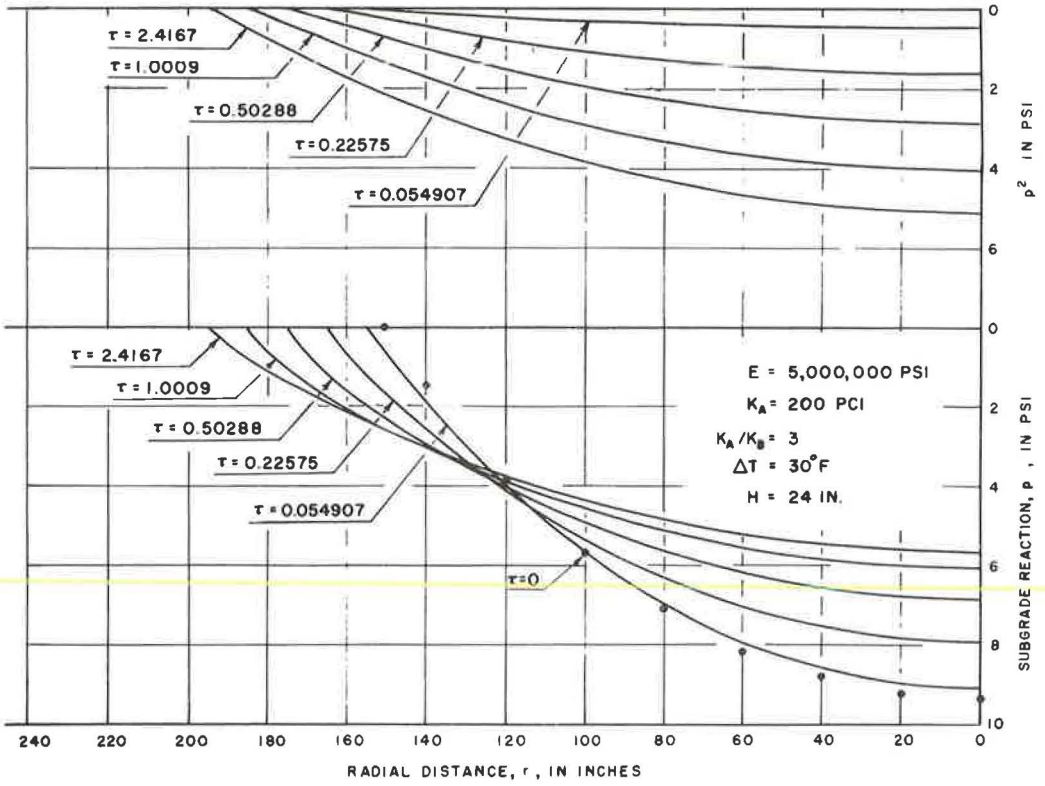

Figure 10. Subgrade reaction and p^2 for slab on standard solid foundation.

given. Eq. 28 gives a temperature distribution that is symmetrical about the mid-depth of the slab. The boundary moment (Eq. 3) is, therefore, zero; hence, this temperature distribution produces only initial stresses (Eq. 4) and no additional warping of the slab results. Because there is no change in geometry, the effects of the temperature distributions defined by Eqs. 27 and 28 are directly additive. For example, with a = 240 in.; H = 12 in.; K = 200 pci; E = 5,000,000 psi:

$$T(y) = \frac{30\,y}{H} - \frac{30\,y^2}{H^2} \tag{29}$$

the initial stress due to the temperature distribution given by Eq. 28 equals (Eq. 4):

$$\sigma_r \text{ (initial)} = \frac{\alpha E}{1-\mu}\left[-T(y) + \frac{1}{H}\int_{-H/2}^{+H/2} T(y)\,dy\right] =$$

$$\frac{\alpha E}{1-\mu}\left[+\frac{30\,y^2}{H^2} - \left(\frac{1}{H}\right)\left(\frac{30}{H^2}\right)\frac{H^3}{12}\right] \tag{30}$$

for $y = -6 = \frac{-H}{2}$ (top surface of slab):

$$\sigma_r \text{ (initial)} = \frac{\alpha E}{1-\mu}\left(+\frac{30}{4} - \frac{30}{12}\right) = \frac{(6 \times 10^{-6})\ (5 \times 10^{6})}{0.85}\left(+\frac{30}{6}\right) = 176.5 \text{ psi (tension)}$$

Therefore, a tensile stress of 176.5 psi is added to the stresses obtained for the linear temperature distribution (at y = -6, top surface of slab) for all values of r and τ. The deflections are identical with those obtained from the linear temperature distribution.

DISCUSSION OF RESULTS

Figure 11 shows the effect of the type of model assumed for the subgrade support on the maximum tensile stress in the slab. For a 24-in. slab on a relatively weak subgrade, the Maxwell model results in a very large reduction in the maximum tensile stress (compared to a Winkler foundation) at a time factor equal to 5. For large values of K_A/K_B, the standard solid model tends towards the Maxwell model; at very small values of K_A/K_B the standard solid model tends towards a Winkler foundation. Thus, in general, the Winkler foundation and the Maxwell model bracket the range in tensile stress likely to occur due to viscoelastic effects in the subgrade. An appropriate standard solid model may be assumed to approximate relaxation effects, as suggested by Freudenthal and Lorsch (24).

The effect of time on the maximum tensile stress in the slab is shown in Figure 12 for a weak subgrade, and in Figure 13 for a relatively strong subgrade. Two important deductions can be made:

1. Viscoelastic effects in the subgrade cause important reductions in maximum tensile stress with time in the case of thick slabs; for thin slabs, relaxation effects are relatively minor and may even result in an increase in the maximum tensile stress with time.
2. For thick slabs, the maximum tensile stresses are significantly lower for slabs on weak subgrades as compared with strong subgrades.

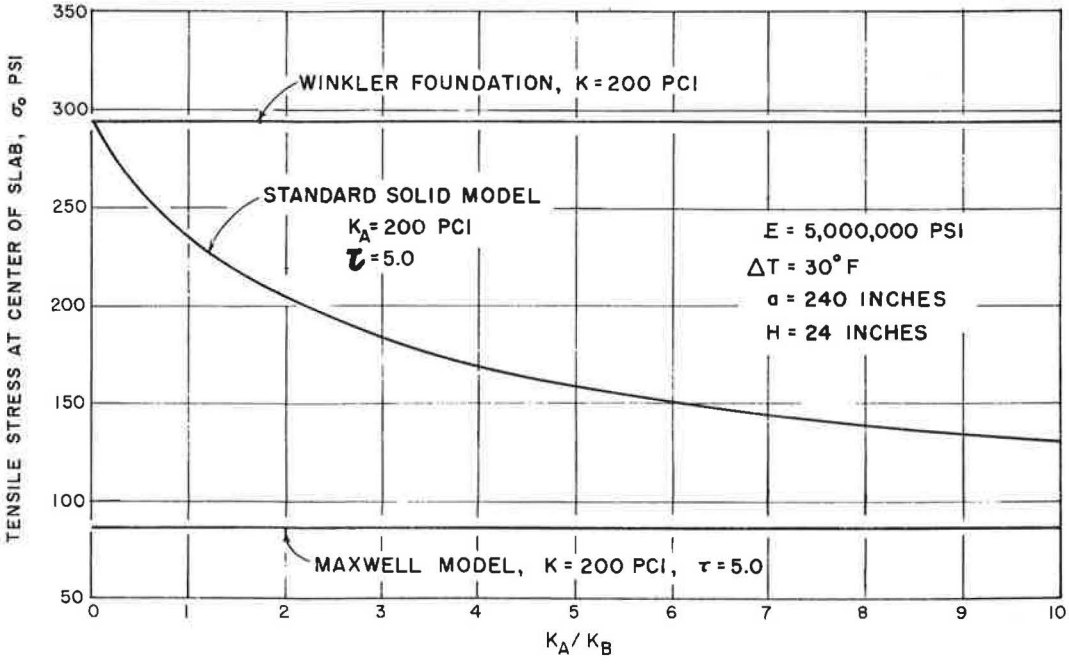

Figure 11. Effect of subgrade support on maximum tensile stress.

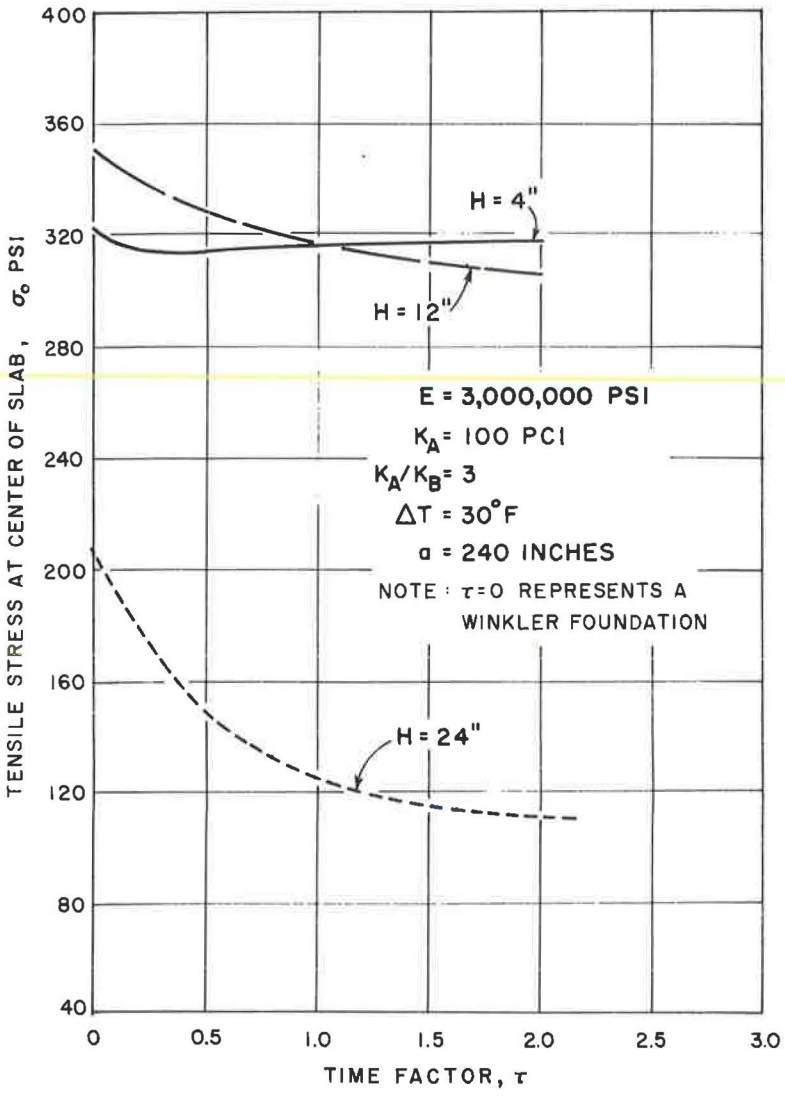

Figure 12. Effect of time on tensile stress at center of slab—standard solid model.

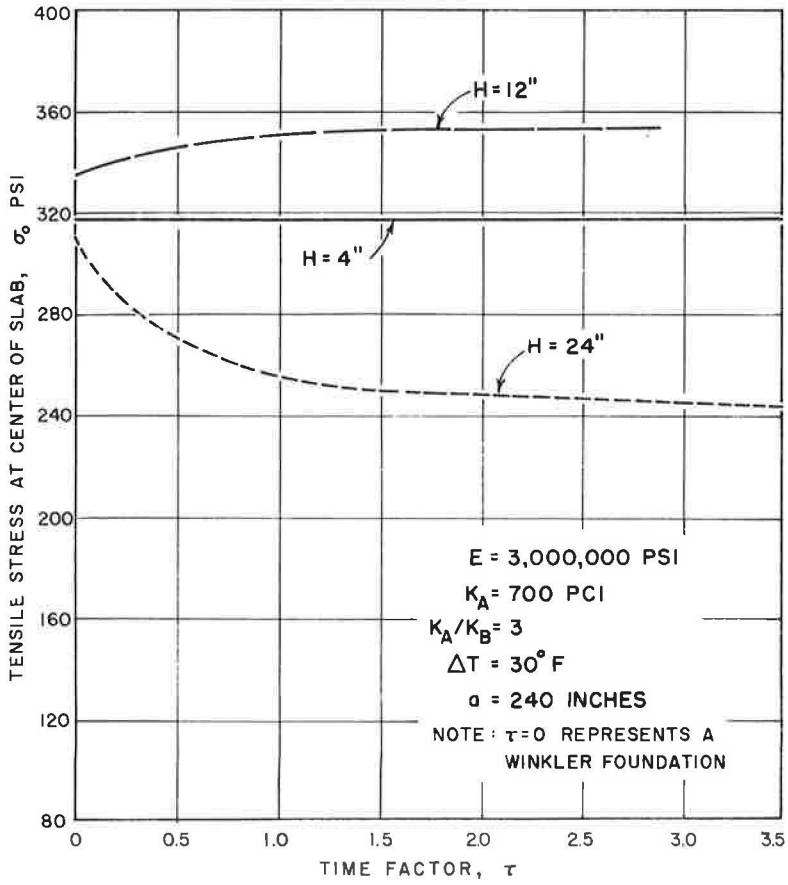

Figure 13. Effect of time on tensile stress at center of slab—standard solid model.

Pending experimental verification of the theoretical results, it appears that the combination of a thick slab and a weak subgrade will combat the detrimental effects of warping most successfully, as shown by Figure 14 where the ratio of the tensile stress at the center of the slab to the modulus of rupture is plotted for the three subgrade models as a function of the modulus of subgrade reaction. For the two viscoelastic models, values of τ were selected so that relaxation is virtually complete (i.e., the slabs have sunk into the ground until they are almost fully supported by the subgrade). Assuming that the standard solid model is a reasonable approximation to reality, it is seen that for thinner slabs little benefit is obtained as the stiffness of the subgrade is increased. This is compatible with performance records obtained at the AASHO Road Test (3). For thick slabs, increased subgrade stiffness is detrimental.

For a given temperature difference between the top and bottom of the slab, a non-linear temperature distribution results in larger tensile stresses than a linear temperature distribution if the gradients in the top half of the slab thickness are larger than in the bottom half (for the case of upward warping) and vice versa for downward warping. Since this type of non-linear temperature distribution commonly occurs in practice (15, 31, 32), the non-linear case is critical from a design standpoint.

The analysis presented herein is sufficiently general to provide a sound basis for significant field experiments. Procedures are available to measure temperature gradients and degree of subgrade support (20); in fact, considerable data on temperature variations have already been accumulated (15, 31, 32). Measurement of the

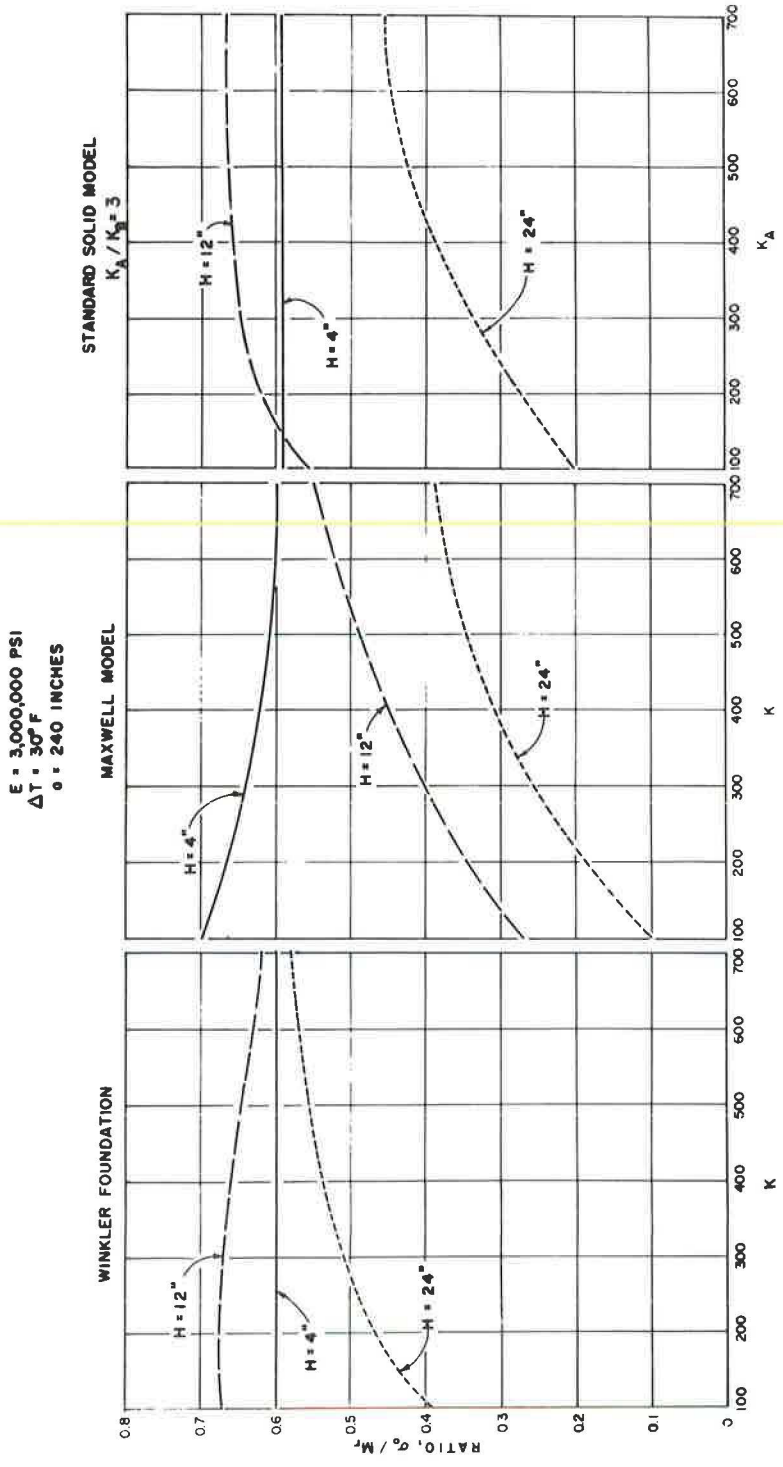

Figure 14. Effect of type and properties of subgrade support on maximum tensile stresses in the slab (relaxation virtually complete).

equivalent effect of transient moisture gradients is a more difficult problem, but considerable progress has recently been made in this connection (41). Experiments to determine the parameters K_A, K_A/K_B, and K_B/θ would permit a full appraisal of the practical utility of the theory presented. Extension of the analysis to account for the effects of moving loads over (partly supported) warped slabs, and for creep effects in the slab itself, would establish the final link between theory and reality in the concrete pavement design problem.

CONCLUSIONS

1. On the basis of the assumptions stated herein, a theory has been developed whereby the stresses, deflections, subgrade reaction, and degree of subgrade support can be computed for finite slabs subject to: (a) warping due to linear or non-linear temperature and/or moisture variations of sufficient magnitude to result in a partly supported slab; and (b) subgrade supports consisting of a Winkler foundation or a standard viscoelastic element.
2. Regardless of the type of subgrade support, thick slabs on weak subgrades develop significantly lower (30 to 80%) tensile stresses due to warping than do thin slabs on weak or strong subgrades, or thick slabs on strong subgrades. Thus, the combination of thick slabs and weak subgrades will combat the detrimental effects of warping most successfully.
3. Viscoelastic effects in the subgrade cause large reductions in the maximum tensile stress with time in the case of thick slabs on weak subgrades; for thin slabs, relaxation effects are relatively minor and may even result in an increase in the maximum tensile stress with time.
4. For a given temperature difference between slab surfaces, non-linear temperature (or moisture) distributions result in larger tensile stresses than linear temperature distributions if the gradients in the top half of the slab are larger than in the bottom half (for the case of upward warping). Since such non-linear temperature distributions are commonly encountered in practice, the non-linear case is critical from a design standpoint.
5. Although predictions based on the new theory are in qualitative agreement with performance records, field experiments are needed (including measurement of the significant parameters involved) to permit a full appraisal of its practical utility.

REFERENCES

1. Farrell, F.B., and Paterick, H.R., "The Capital Investment in Highways." HRB Proc. 32:1 (1953).
2. "Highway Statistics." U.S. Bureau of Public Roads, Washington (1960).
3. "The AASHO Road Test, Report 5, Pavement Research." HRB Special Report 61E (1962).
4. Harr, M.E., and Leonards, G.A., "Warping Stresses and Deflections in Concrete Pavements." HRB Proc. 38:286 (1959).
5. Goldbeck, A.T., "Thickness of Concrete Slabs." Public Roads, Vol. 1 (1919).
6. Older, C., "The Design of Rigid Pavements." Concrete, Vol. 18 (1921).
7. Westergaard, H.M., "Stresses in Concrete Pavements Computed by Theoretical Analyses." Public Roads (April 1926).
8. Westergaard, H.M., "Analysis of Stresses in Concrete Roads Caused by Variations of Temperature." Public Roads (May 1927).
9. Sparkes, F.N., "Stresses in Concrete Road Slabs." Structural Engineer, 17:II, 98-116 (1939).
10. Bradbury, R.D., "Reinforced Concrete Pavements." Wire Reinforcement Institute, Washington (1938).
11. "Concrete Pavement Design." Portland Cement Association, Chicago (1951).
12. Sparkes, F.N., and Smith, A.F., "Concrete Roads." Edward Arnold Co., London (1952).
13. Kelly, E.F., "Applications of the Results of Research to the Structural Design of Concrete Pavements." Public Roads, Vol. 20 (1939).

14. Spangler, M.G., "Stresses in the Corner Region of Concrete Pavements." Iowa Eng. Expt. Sta. Bull. 157 (1942).
15. Teller, L.W., and Sutherland, E.C., "The Structural Design of Concrete Pavements." Public Roads (Oct., Nov., Dec. 1935; Sept., Oct. 1936; Apr., May, June 1943).
16. Winkler, E., "Die Lehre von Elastizitat und Festigkeit." Prag (1867).
17. Terzaghi, K., "Evaluation of Coefficients of Subgrade Reaction." Geotechnique, 5:4:297 (Dec. 1955).
18. Gorbounov-Possadov, M.I., "Beams and Slabs on an Elastic Base." Mashstroyizdat, Moscow (1949). Also, "Tables for the Design of Thin Slabs on Elastic Foundations." Moscow (1959).
19. Hetenyi, M., "Beams on Elastic Foundation." Univ. of Michigan Press, Ann Arbor (1946).
20. Wiseman, J.F., Harr, M.E., and Leonards, G.A., "Warping Stresses and Deflections in Concrete Pavements: Part II." HRB Proc. 39:157 (1960).
21. Tan, T.K., "Secondary Time Effects and Consolidation of Clays." Academia Sinica, Inst. of Civil Eng. and Arch., Harbin, China (June 1957).
22. Lo, K.Y., "Secondary Compression of Clays." Jour., Soil Mech. and Fdn. Division, ASCE, 87:4:61 (Aug. 1961).
23. Freudenthal, A.M., "The Inelastic Behaviour of Engineering Materials and Structures." Wiley (1950).
24. Freudenthal, A.M., and Lorsch, H.G., "The Infinite Elastic Beam on a Linear Viscoelastic Foundation." Jour. of the Engineering Mech. Div., ASCE Proc. (Jan. 1957).
25. Hoskin, B.C., and Lee, E.H., "Flexible Surfaces on Viscoelastic Subgrades." Journ. of the Engineering Mech. Div., ASCE Proc. (Oct. 1959). "The Analysis of Loaded Flexible Surfaces over Subgrades with Viscoelastic Material." Tech. Rpt. No. 5 (Final), Division of Applied Mechanics, Brown Univ. (July 1958).
26. Pister, K.S., and Williams, M.L., "Bending of Plates on a Viscoelastic Foundation." Jour. of the Engineering Mech. Div., ASCE Proc. (Oct. 1960).
27. Reissner, E., "A Note on Deflections of Plates on a Viscoelastic Foundation." Jour. of Applied Mechanics, 25:1 (March 1958).
28. Kerr, A.D., "Viscoelastic Winkler Foundation with Shear Interactions." Jour. of the Engineering Mech. Div., ASCE Proc. (June 1961).
29. Lee, E.H., "Viscoelastic Stress Analysis." Proc. of the First Symposium on Naval Structural Mechanics, Pergamon Press (1960).
30. Boley, B.A., and Weiner, J.H., "Theory of Thermal Stresses." Wiley (1960).
31. Lang, F.C., "Investigational Concrete Pavement in Minnesota." HRB Proc., 20:348 (1940).
32. Corps of Engineers, U.S. Army, Ohio Division Laboratories, "Stresses in Thick Concrete Slabs Due to Curved Temperature Gradient." Lockborne No. 2 — 300,000 Pound Experimental Mat, August 1947.
33. Thomlinson, J., "Temperature Variations and Consequent Stresses Produced by Daily and Seasonal Temperature Cycles in Concrete Slabs." Conc. and Construction Engineering (1940).
34. Timoshenko, S., and Goodier, J.N., "Theory of Elasticity." McGraw-Hill (1951).
35. Timoshenko, S., and Woinowsky-Krieger, S., "Theory of Plates and Shells." McGraw-Hill (1959).
36. Colatz, L., "Numerische Behandlung Von Differentialgleichungen." Springer-Verlag, Berlin (1955).
37. Hildebrand, F.B., "Introduction to Numerical Analysis." McGraw-Hill (1956).
38. Reddy, A.S., "Time Dependent Warping Stresses and Deflections in Slabs on Ground." Ph.D. Thesis, Purdue Univ. (Jan. 1963).
39. McCracken, D.D., A Guide to FORTRAN Programming. Wiley (1961).
40. Leonards, G.A., and Harr, M.E., "Analysis of Concrete Slabs on Ground. Jour., Soil Mech. and Fdn. Division, ASCE, 87:4:35 (1959).
41. Bell, J.R., "A Study of the Dielectric Properties of Hardened Concrete with Respect to Their Utility as Moisture Indicators.", Ph. D. Thesis, Purdue Univ. (Jan. 1963).